

HIGH RESOLUTION BEAM PROFILE MONITORS IN THE SLC*

M. C. ROSS, J. T. SEEMAN, R. K. JOBE, J. C. SHEPPARD, R. F. STIENING

Stanford Linear Accelerator Center
Stanford University, Stanford, California, 94305

ABSTRACT

In the SLC linac, low emittance beams with typical transverse dimensions less than 0.2 mm must be accelerated without effective emittance growth. In order to monitor this we have installed a high resolution beam profile monitor system which consists of an aluminum target covered with a fine-grained phosphor, a magnifying optical system, a television camera and video signal recording electronics. The image formed when the beam strikes the phosphor screen is viewed on a CRT monitor at the console and selected horizontal and vertical slices of the beam spot intensity are recorded. A 20 MHz transient waveform recorder is used to sample and digitize the raw video signal along the selected slice. The beam width is determined by fitting the background subtracted data to a Gaussian. Beam spots less than 6×3 mm can be viewed. Beam spot sizes $\sigma_{x,y} < 80 \mu m$ have been measured.

SYSTEM REQUIREMENTS

Accurate beam profile measurements are used in the SLC to determine emittance (ϵ), optical parameters (β, α) and energy spread^{1,2,3}. With typical transverse beam sizes of less than 0.2 mm system resolution must be kept small ($\sigma_{sys} \leq .05$ mm). This is especially important since the emittance depends on the square of the beam size

$$\epsilon = \sigma^2 / \beta$$

so that errors made in the determination of ϵ are very sensitive to errors made in the measurement of the beam size ($\sigma_{x,y}$).

It is useful to characterize the systematic error made in the determination of $\sigma_{x,y}$ as σ_{sys} , the width which would be seen if the beam spot was infinitely small. In an imaging system, such as this one, an estimate of σ_{sys} can be made by evaluating the performance of each element in the data acquisition chain in terms of a spatial bandpass function (also known as modulation transfer function). The total system transfer function is given by the product of the component functions. In this way, diffraction, image sensing electronic and signal processing electronic effects are taken into account. A good way to estimate σ_{sys} is to approximate the system transfer function as a Gaussian. The measured width σ_m is related to the actual beam size (σ_r) and σ_{sys} by

$$\sigma_m^2 = \sigma_r^2 + \sigma_{sys}^2.$$

The effect of σ_{sys} on the the determination of ϵ depends on both the beam size and optics.

The method⁴ used to determine ϵ is to adjust the focusing upstream of the fluorescent screen causing the square of the beam size to trace out a parabola

$$\sigma^2 = \sigma_0^2 R_{12}^2 (K - K_0)^2 + \frac{R_{12}^2 \epsilon^2}{\sigma_0^2}$$

* Work supported by the Department of Energy, contract DE-AC03-76SF00515.

where σ_0 is the beam size in the upstream quadrupole of strength K , R_{ij} are the transfer matrix elements between the quadrupole and the screen,

$$K_0 = -\frac{\sigma_{11} R_{11} + \sigma_{12} R_{12}}{\sigma_{11} R_{12}}$$

is the quadrupole strength at the minimum of the parabola, and σ_{ij} are the beam size and divergence matrix elements⁵ at the quadrupole ($\sigma_0^2 = \sigma_{11}$). Emittance data can also be processed using an analysis program which extends this technique so that more than one upstream quadrupole may be varied.

Since σ_{sys} contributes to the observed width in quadrature we see that it does not affect the determination of σ_0 and K_0 . However it makes a contribution to the observed emittance,

$$\epsilon_m = \sqrt{\frac{\sigma_0^2 \sigma_{sys}^2}{R_{12}^2} + \epsilon_r^2}.$$

For example, a system resolution of $100 \mu m$ will cause $\epsilon_m = 1.5 \epsilon_r$ for a 10 GeV SLC beam ($\beta_0 = 10 m$, $\gamma \epsilon_r = 3 \times 10^{-5} m-rad$). It is clear from the above expression that the requirements made on the performance of the profile monitor can be relaxed somewhat by placing it in an appropriate location.

SYSTEM OVERVIEW

Figure 1 is the profile monitor system schematic. Each of the components: screen, camera optics, tube, amplifier, cable transmission and digitizing signal processors can affect σ_{sys} in the same way that circuit elements can affect the impulse response of a circuit. However, the optics, camera tube and transmission cable contribute the most to σ_{sys} .

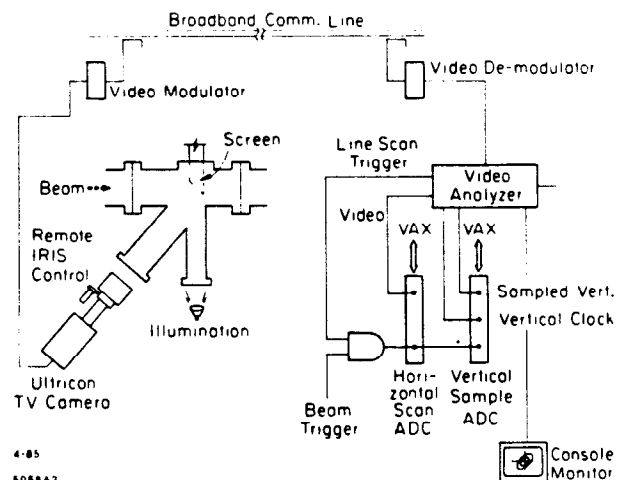


Fig. 1. Profile monitor system schematic. A fine-grained fluorescent screen is viewed by a diode array CCTV camera. The signal passes over a broadband cable to the control center where selected horizontal and vertical slices are digitized.

Figure 2 shows the mechanical construction of the profile monitor. The screen itself, shown in the inset, has an active area of 4.2 mm vertical by 6 mm horizontal surrounded by an array of holes used for scale. The plane of the screen makes a 45 degree angle with the vertical plane so that the vertical active area is compressed to 3 mm. The screen insertion mechanism forces the holder upon a shallow tapered stop ensuring that the inserted position is reproducible. The phosphor, $Gd_2O_2S:Tb$, is settled on the aluminum in a water bath and bound to it with barium silicate⁶. This technique is used by the CRT industry and results in a very fine grained screen.

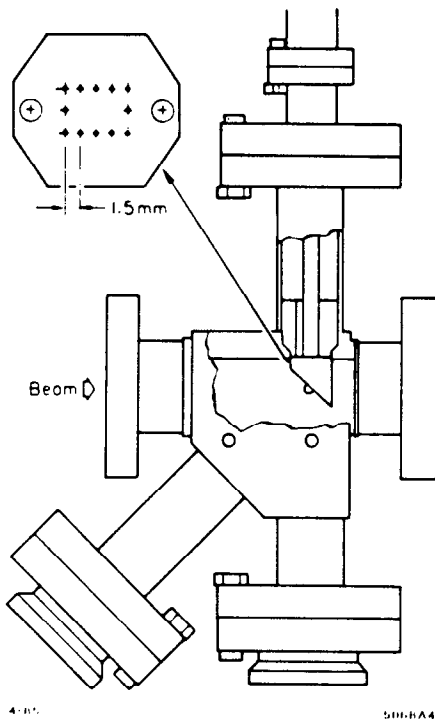


Fig. 2. Mechanical construction of the high resolution profile monitor. Illumination (for calibration purposes) enters through the port directly below the screen and the image is viewed through the lower left port.

The screens have been tested for linearity and sensitivity to radiation damage using the linac beam. No sign of radiation damage was observed after bombardment with 1.6×10^{15} electrons in a 0.5 mm spot. Some damage was seen at three times this intensity. Linearity tests showed no indication of saturation for beam spots of 10^{10} particles in a 100 μm spot.

The screen is viewed with a diode array image tube television camera (72 diodes/mm)⁷. Typical camera performance contributes $60 \mu m/M$ to σ_{sys} where M is the magnification of the camera optics. The .7 inch camera tube has an active area of 8.8×6.6 mm, setting $M = 1.5$. The linearity of the diode array camera is very good and it exhibits none of the image burn in and saturation characteristic of amorphous photoconductor (vidicon) cameras. A 135 mm focal length telephoto⁸ lens with remote iris control is used to focus the image and control the signal strength on the camera tube. Careful focusing and iris adjustment are required in order to keep this part of the system from contributing most of σ_{sys} .

The closed circuit television signal is transmitted on the SLC broadband communications cable to the control center. There it is received by an ordinary television receiver and passed to a video analyzer⁹ which is used to select a horizontal and a vertical sampling line. The analyzer provides, under front panel control, both a trigger pulse which can be used to select a particular horizontal scan line and a composite vertical signal made up by sampling each horizontal scan once at a particular point along the scan. The vertical signal is accompanied with a synchronized clock. Horizontal and vertical slices of the image are digitized in two high speed transient waveform digitizers. Both are gated with the machine beam time trigger and record the waveform with 8 bit resolution at 256 points. The data are then read out through CAMAC by the SLC control system into the main control computer (VAX).

Background data are taken with the beam suppressed and subtracted from the beam on data. The result is scanned for signal and fit to a Gaussian. Spatial calibration constants (digitizations/mm) are either retrieved from the database or manually set using the pattern of holes on the screen. Since each emittance measurement consists of several beam size measurements made at different quadrupole settings, selected magnet strengths are recorded as the data is taken and accepted. Emittance and other beam parameters are determined using the full optics deck for that part of the system.

SYSTEM PERFORMANCE

Figure 3 shows two examples of single pulse digitized data from a screen at the 1.2 GeV point in the SLC injector. The online fit is shown superimposed on the data. These clearly show the non-Gaussian nature of the beam emerging from the SLC gun at currents of 3×10^{10} . Figure 4 shows σ^2 vs. the strength of an upstream quadrupole. The error bars are the weighted average of the errors on the fit σ for several (typically five) measurements and represent only statistical errors.

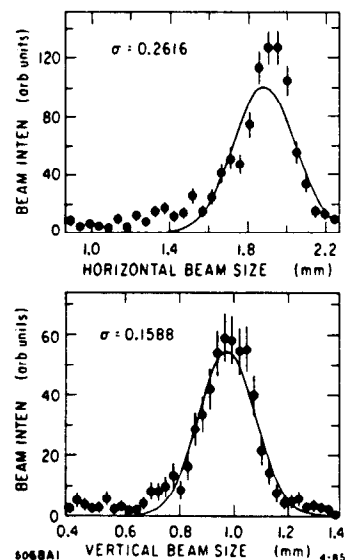


Fig. 3. Background-subtracted profile data taken at the 1.2 GeV point in the SLC injector. The online fit is shown superimposed on the data with the fit result for the width (σ) shown in the corner.

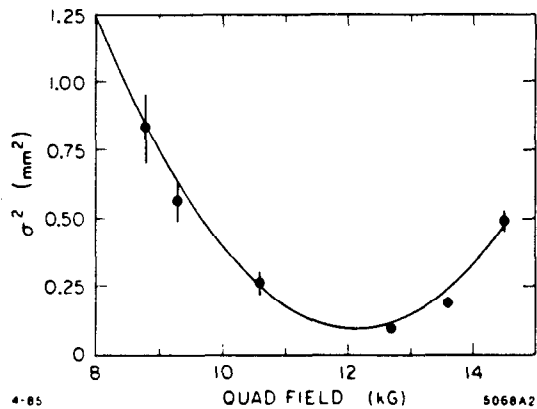


Fig. 4. Square of beam size (σ^2) versus strength of an upstream focusing magnet. The curve is the parabolic least squares fit to the data.

The optics contribute about $50\mu m$ to σ_{yy} , with the iris optimally set (midrange in most lenses). This combined with the contribution from the camera gives $\sigma_{yy} = 68\mu m$. At the profile monitor located just after the extraction point from

the damping ring, beam spots as small as $80\mu m$ have been seen. At that point adjustment of the quadrupole caused no further decrease in the apparent beam size, indicating that $\sigma_{yy} = 80\mu m$ is in good agreement with the expected value.

A development program is underway to push this limit lower. By decreasing the scale of the device (smaller lens to screen distance) and improving the lens focusing procedure, we expect to achieve $\sigma_{yy} = 30\mu m$. At this level, the grain size of the phosphor may become an important factor.

REFERENCES

1. J. C. Sheppard *et al.*, Proc. 1984 Linear Accelerator Conf., GSI-84-11, 1984.
2. M. C. Ross *et al.*, these proceedings.
3. J. T. Seeman *et al.*, these proceedings.
4. J. C. Sheppard *et al.*, *IEEE Trans. Nucl. Sci.* NS-30, 2161 (1983).
5. K. L. Brown *et al.*, TRANSPORT, SLAC-91, 1977.
6. GTE/Sylvania, Towanda, PA.
7. RCA Ultricon, AN-6994, Lancaster, PA.
8. Nikon Inc., Garden City, NY.
9. Colorado Video Inc., Boulder, CO.